RESEARCH ARTICLE

European Journal of Advanced Chemistry Research
www.ej-chem.org

Poly Acrylic-Chitosan Co-Polymer as Corrosion Inhibitor for Mild Steel in 0.5 M Hydrochloric Acid Solutions

Sani Nazifi Dalhatu, Kolo Alhaji Modu, Auwal Adamu, Mahmoud, Harami Malgwi Adamu, Suleiman Yusif Sule, Ridwanu Murtala, Faiz Abdulkadir SheShe, and Hamza Badamasi

ABSTRACT

Corrosion prevention has been one of the major concerns these days various methods have been adopted for corrosion prevention. However, the use of corrosion inhibitors has proven to be the easiest and cheapest method for corrosion prevention. But then most of the conventional inhibitors are expensive and toxic. Therefore the recent focus has been turned to developing non-toxic and cheap corrosion inhibitors. To achieve that a Polyacrylic acid was successfully grafted on chitosan by the thermal method using a reflux condenser. This copolymer was characterized by FTIR, TGA, and XPS. The corrosion inhibition performance of the grafted polymer was tested on mild steel in 0.5 M HCl under different conditions by gravimetric method. Mild steel coupon was analyzed using SEM to understand the effect of the inhibitor on the mild steel corrosion. The results were subjected to various adsorption isotherm models to understand the corrosion mechanism. The weight loss results show high inhibition efficiency of 86.50432 % for 24 hrs. Immersion time at 300 °C conditions. Data best fitted with Langmuir adsorption model with a good correlation coefficient of 0.9933.

Keywords: Chitosan, Co-Polymer, Corrosion Inhibitor, Mild Steel, Poly Acrylic Acid, SEM, XPS.

Published Online: October 28, 2022

ISSN: 2684-4478

DOI: 10.24018/ejchem.2022.3.3.101

S. N. Dalhatu*
Department of Chemistry, Faculty of Science, Kano State University of Science and Technology Wudil, Nigeria.
(e-mail: snimam268@gmail.com)

K. A. Modu
Department of Chemistry, Faculty of Science, Abubakar Tafawa Balewa University Bauchi, Nigeria.
(e-mail: amodukolo@gmail.com)

A. A. Mahmoud
Department of Chemistry, Faculty of Science, Abubakar Tafawa Balewa University Bauchi, Nigeria.
(e-mail: aamahmoud@atbu.edu.ng)

H. M. Adamu
Department of Chemistry, Faculty of Science, Abubakar Tafawa Balewa University Bauchi, Nigeria.
(e-mail: hmadamu@atbu.edu.ng)

S. Y. Sule
Department of Chemistry, Faculty of Science, Kano State University of Science and Technology Wudil, Nigeria.
(e-mail: sysule@kustwudil.edu.ng)

R. Murtala
Department of Chemistry, Faculty of Science, Kano State University of Science and Technology Wudil, Nigeria.
(e-mail: ridwanmo@yahoo.com)

F. A. SheShe
Department of Chemistry, Faculty of Science, Kano State University of Science and Technology Wudil, Nigeria.
(e-mail: fasheshe@gmail.com)

H. Badamasi
Department of Chemistry, Faculty of Science, Federal University Dutse, Nigeria.
(e-mail: hamza.badamasi@fud.edu.ng)

****Corresponding Author***

I. INTRODUCTION

Mild steels are frequently used to manufacture different equipment in many, due to economical and have suitable mechanical properties in many industrial applications. Major challenge of using the mild steel is mild steel was prone to the corrosion often exposure to corrosive environments [1]. Nowadays, corrosion has become one of the major problems for facing many industries and many nations [2]. Corrosion inhibition is recognized as one of the easiest and most effective methods for corrosion mitigation. Inhibition

European Journal of Advanced Chemistry Research
www.ej-chem.org

science started in the 1930s, this technology has changed and developed over the last decades [3]. Several efforts have been made to convert the challenge of corrosion by many researchers, and the use of corrosion inhibitors is one of the most economical and practical means of controlling metallic corrosion in different corrosive media [2]. But then most conventional corrosion inhibitors are toxic and expensive [4]. Therefore Interest in the use of natural materials as corrosion inhibitors is a subject of interest by many academics. Chitosan has been reported as a good corrosion inhibitor by some researchers. Still, the intensive inter and intermolecular hydrogen bonding of this polymer reduced its solubility in an aqueous and acidic environment hence reducing its inhibition efficiency [5]. In this research, Chitosan was modified with polyacrylic acid and used as an inhibitor for mild steel in Hydrochloric acid to optimize the inhibition efficiency of the polymer.

II. Materials and Methods

A. Materials

Chitosan of medium molecular weight was purchased from Sigma Aldrich, Acrylic acid monomer from Aldrich, tert-Butyl hydroperoxide, 70 % solution in water was purchased from Acros Organics, Hydrochloric acid from sigma Aldrich, other reagents such as acetone, ethanol, were of analytical grade and used without further purification. Mild steel coupons and emery paper were collected from Khon kaen University workshop.

B. Methods

Monomer purification was done according to previously reported [6]. The grafting of chitosan was carried out in reflux at 120 °C for two hours in this reaction 0.5 grams of chitosan was dissolved in 50 ml of 0.1M acetic acid solution, afterward, 0.5 ml of 70 % solution of tertiary butyl hydroperoxide in water was added as initiator, and this mixture was then stirred on a magnetic stirrer for 20 minutes to homogenize the mixture, 0.5 ml of monomer (acrylic acid) was added and then the whole mixture was then poured into the reflux condenser on a magnetic stirrer for 120 minutes at 120 °C and stirred at 250 rpm. The mixture turned to reddish and then white color at the end of the reaction, the copolymer was precipitated in acetone and filtered with Whitman filter paper, and then extracted in a soxhlet extractor with deionized water for 2 hours to remove unreacted acrylic acid and solvent. The Cs-g-PAA was then dried in the ovum at 60 °C for 4 hours. This procedure was repeated under different conditions to optimize the yield.

C. Characterization

FT-IR was obtained using FTIR infrared spectrophotometer model; Tensor27 S/N; 3683 (broker Hong Kong limited). The surface morphologies were imaged using the scanning electron microscope (SEM) model SNE4500M South Coria, Thermal analysis was carried out using Hitachi TG/DTA thermogravimetric analyzer instrument model no. STA7200 Hitachi, using the scan rate of 100C/min range 25 °C to 600 °C, the change in the binding energy of various atoms was determined using XPS Thermo Kalpha, ESCALAB 250XI, Axis Ultra DLD Kratos AXIS SUPRA, PHI-5000 versaprobe III.

D. Corrosion Analysis

The corrosion analysis was performed using weight loss [7], [8] and electrochemical methods [9], [10].

III. Results and Discussion

A. Characterizations

1) Fourier transform infrared spectroscopy (FTIR)

Fig. 1 shows the FTIR spectrum of (a) chitosan with broadband at 3355 cm-1 which corresponds to stretching vibration of O-H and N-H overlapping to each other this is in agreement with [11]. Two 1591 cm^{-1} and 1603 cm^{-1} correspond to the stretching of amide I and amide II bands [6]. The band at 1025 cm^{-1} is assigned to β(1-4)glucoside bond which is characteristic of polysaccharide chitosan structure[12]. The FTIR spectrum of Cs-g-PAA with the subsequent shift from 1700 cm^{-1} to 1735 cm^{-1} (in pure PAA spectrum) is a shred of evidence that PAA was grafted on the chitosan, sharp intense peak at 1450 cm^{-1}, the disappearance of O-H bending peaks of primary alcohol around 1000 cm^{-1} on the Cs-g-PAA spectrum is an indication that primary alcohol in chitosan participated in the reaction [13].

2) Thermal analysis

The thermogravimetric (TG) curve of chitosan and Cs-g-Paa in Fig. 2 shows a two-stage degradation pattern. The first weight loss of 6.58 % around 100 °C for Chitosan is attributed to the evaporation of water [14] There was a sharp weight loss (51.47 %) around 297-450 °C this is due to depolymerization of chitosan

and the decomposition of the amine group of the chitosan [6]. On the other hand, the Cs-g-Paa thermogram shows first-step weight loss (13.25 %) around 90 °C to 250 °C, which is associated with loss of water and decomposition of polyacrylic acid from the chitosan backbone [6]. The second degradation step was observed from 280 °C to 450 °C. DTA of pure Cs recorded in air show a sharp exothermic peak around 300 °C which is accompanying thermal pyrolysis of the chitosan, and thermal decomposition of amino and N-acetyl residues [15]. Similarly, the Cs-g-Paa curve shows a less intense exothermic peak around 290 °C. DTG of pure Chitosan exhibited maximum thermal decomposition temperature (T_{max}) at 300 °C. However, Cs-g-Paa has T_{max} around 279 °C (260.90 µg/min). The DTG maxima temperature order is the same as found in DTA Curve. The results from the thermal analysis indicate that grafting with polyacrylic results in decreases in the thermal stability of the polymer [16]. This can be explained this way, in the pure chitosan structure there is an extensive intermolecular hydrogen bond, so to graft acrylic acid on the chitosan, the cluster of this hydrogen must be distorted by inserting acrylic acid between these molecules.

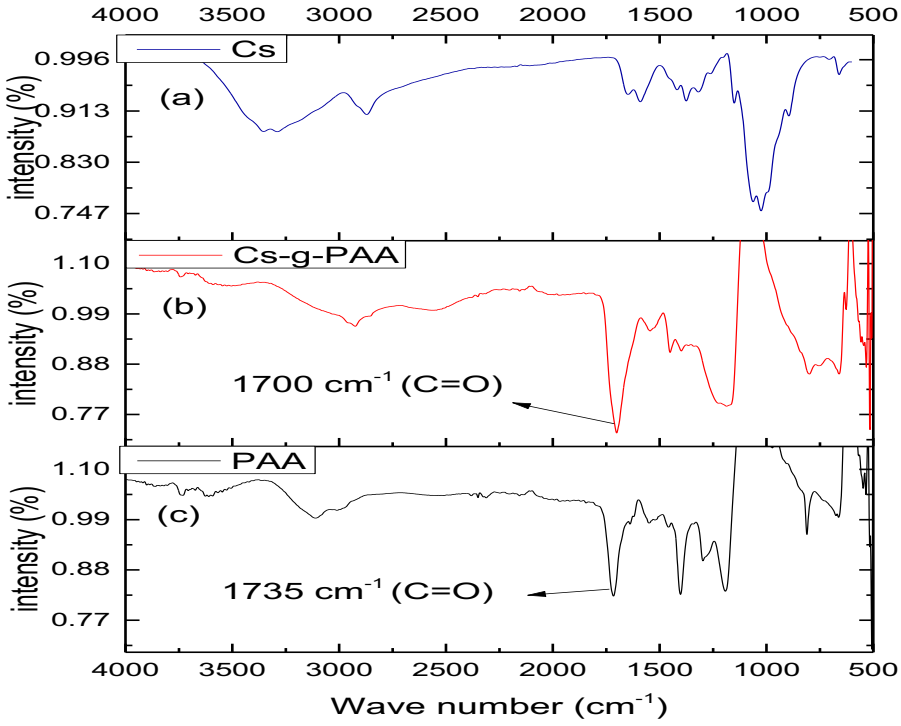

Fig.1. Attenuated Fourier Transform Infrared Spectra of (a) Chitosan and (b) Cs-g-Paa and (c) Poly-acrylic acid.

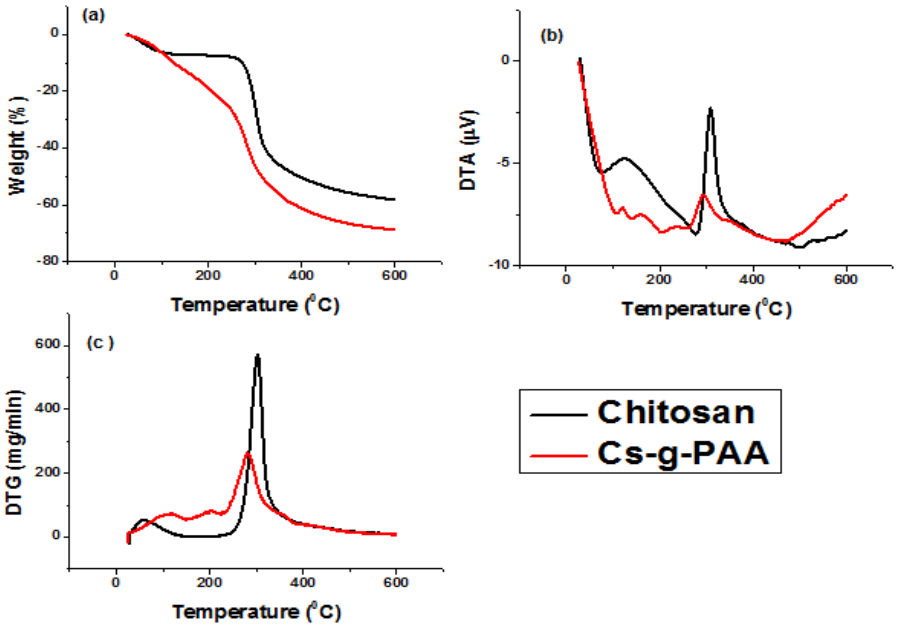

Fig. 2. Thermal analysis of (a) TGA (b) DTA and (c) DTG.

3) X-ray photon spectroscopy (XPS)

The deconvolution of the peak from the XPS spectrum of Cs-g-Paa for each element that existed on its surface was carried out to investigate the sub-peak component using the Gaussian–Lorentzian function based on theoretical prediction and previously reported works from the origin lab software [17]. The C 1s peak for Cs-g-Paa Fig. 3a was resolved into C–C bonds, C–O or C–O–C bonds and, C=O with respective binding energy as 284.3 eV, 286.3 eV, and 288.2 eV. The presence of C=O on the surface of Cs-g-Paa is another indication that Paa was successfully grafted on the chitosan. The N 1s peak Fig. 3b was deconvoluted into two sub-peaks at 399.7 eV corresponding to primary amine (C-NH_2), and 401.27 eV, which were assigned secondary amine (C-NH), deconvoluted N 1s show that some of the grafting processes occur through amine group and the grafting for amine group is high looking at the intensity of the secondary amine peak. The O 1s spectra Fig. 3c for Cs-g-Paa were deconvoluted into two sub-peaks at 531.1 eV and 532.5 eV Representing C–O or C–O–C and C=O bonds, respectively [18]. 3.2.0 Weight loss.

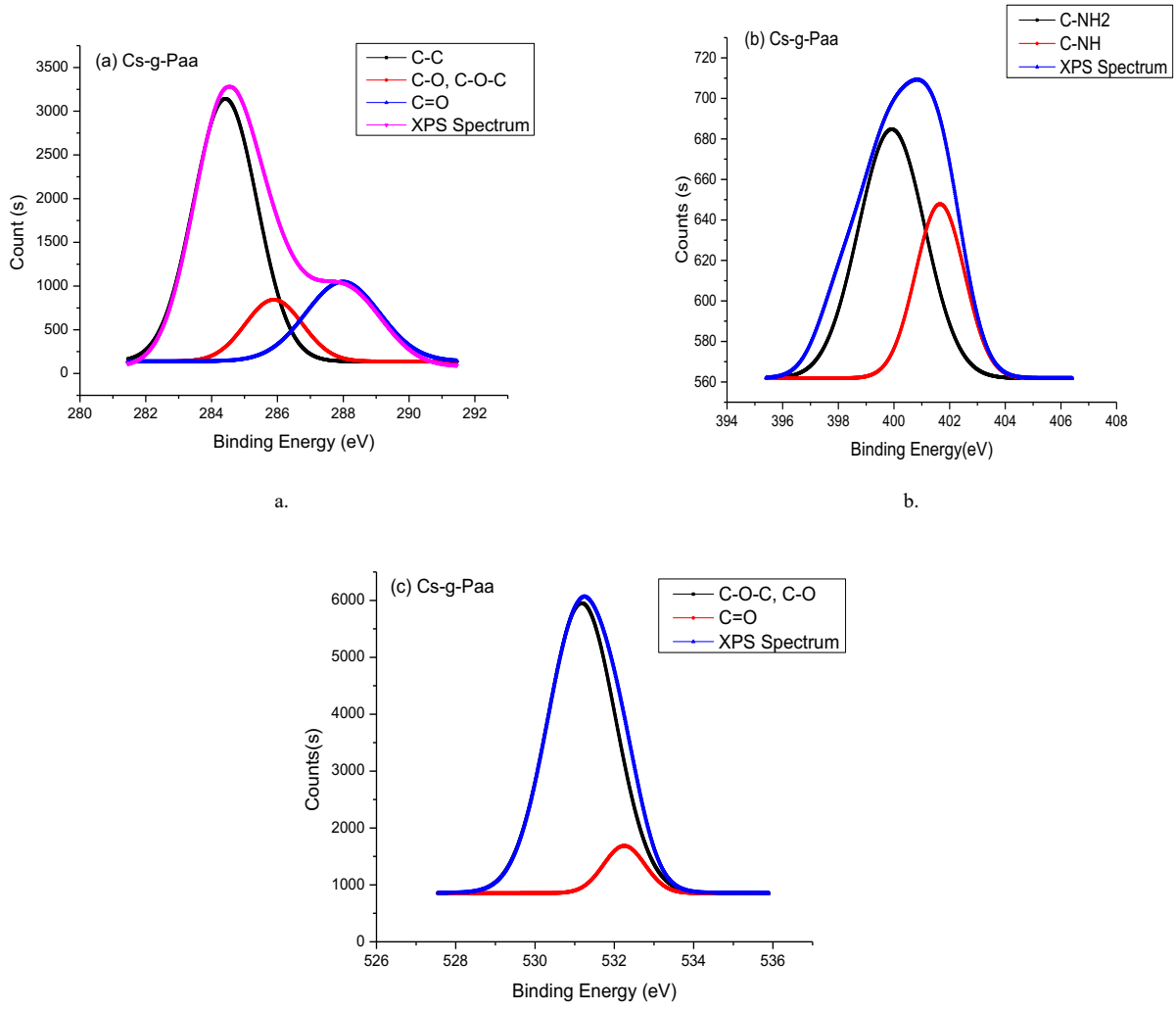

Fig. 3. X-Ray Photon Spectroscopy XPS; a) 1s C, b) 1s N, and c) 1s O.

B. Corrosion Rate and Inhibition Efficiency

The extent of the corrosion process at different conditions can be presented in terms of corrosion rate, inhibition efficiencies, the extent of surface coverage and weight loss. The corrosion at a given condition was related to weight loss in the sense that increasing the concentration of each inhibitor was associated with decreases in corrosion rate. The inhibition efficiency shows the capacity of each inhibitor in preventing the corrosion process; it is more related to the surface coverage. These parameters have been studied under different reaction conditions to optimize the inhibition of each inhibitor. The effect of immersion time, inhibitor dose, and temperature on corrosion rate and inhibition efficiency were presented in table 1. The inhibition efficiency varies linearly with inhibitor concentration, and this could be due to the fact that at lower concentration there exist a large surface that will not be covered by the inhibitor molecule. On

increasing the concentration of inhibitor the surface coverage increases up to the level where the surface will be covered completely [19]. The inhibition efficiency decreases with increases in time of contact and temperature. For immersion time, at the early stages chances of adsorption is very high and there is a limited chance for desorption [20]. Thus as time goes the extent of inhibition will be reduced. The effect of temperature on corrosion rate shows an increase in temperature resulting in the decrease in inhibition efficiency of the polymer. This is because raising temperature demotes the adsorption of inhibitors and at the same time, promotes the mild steel dissolution process [21]. Similarly, the inhibition efficiency decreases as the temperature was raised, and this is because various changes on the metal surface can occur in inhibition reactions at high temperatures, such as fast etching, rupture, desorption of inhibitor, and even rearrangement of the inhibitor, this observation is frequent with most organic inhibitors [22].

TABLE I: CORROSION RATE AND INHIBITION EFFICIENCY

Immersion Time (Hours)	Cr ($gh^{-1}cm^2$)	θ	IE (%)
2	0.000896	0.921334	92.13341 ± 1.23
4	0.000734	0.904464	90.44642 ± 2.24
6	0.000705	0.895714	89.57138 ± 3.74
8	0.000731	0.883591	88.35905 ± 1.96
12	0.000721	0.875282	87.52822 ± 3.19
24	0.000627	0.865043	86.50432 ± 2.54
Inhibitor concentration			
100	0.00136	0.707086	70.7086 ± 2.421
200	0.001153	0.751701	75.17011± 3.21
300	0.000923	0.801196	80.11964 ± 1.32
400	0.000731	0.842558	84.25579 ± 2.32
500	0.000627	0.865043	86.50432 ± 2.43
Temperature (K)			
325	0.002577	0.752427	75.24266 ± 3.15
313	0.001427	0.805356	80.53561 ± 2.14
308	0.000884	0.836383	83.63835 ± 2.21
303	0.000627	0.865043	86.50432 ± 1.12

TABLE II: LANGMUIR ADSORPTION PARAMETERS

Intercept	1/int	log1/int	lo(1/55.5)	logx-k	RT	ΔG	(kj
30.36976	0.032927	-1.48244	-1.74429	-0.26185	2519.142	-659.641	-0.65964

C. Adsorption Model

Langmuir adsorption: Various adsorption isotherm models such as Temkin, Flory-Huggins, El-awady, Frumkin Freundlich and Langmuir were tested on the surface area coverage values, the adsorption process was well fitted with Freundlich and Langmuir adsorption, with a very good correlation coefficient of 0.96423 and 0.98657 respectively. The adsorption was not fitted with Temkin, Flory-Huggins, El-awady, and Frumkin having the correlation coefficient of 0.48389, 0.29538, 0.41659, and 0.7566 respectively. Langmuir adsorption isotherm being the best-fitted model is represented by (1) [23].

$$\frac{C}{\theta} = \frac{1}{K_{ads}} + C \tag{1}$$

Where, K and C represent the equilibrium constant of the adsorption process and Inhibitor concentrations, respectively. A plot of C/θ Vs C gives a straight line with slope = $1/K_{ads}$ and intercept = C this was depicted in figure 16. The equilibrium constant of adsorption K_{ads} is related to the standard Gibs free energy of adsorption ΔG^0_{ads} by (2) [24].

$$K_{ads} = \frac{1}{55.5}\, exp^{-\Delta Gads/RT} \tag{2}$$

The logarithmic form of (2) is given by (3).

$$logK_{ads} = \frac{log1}{55.5} - \frac{\Delta Gads}{RT} \tag{3}$$

Where 55.5 is the concentration of water in the solution in mol/L, R is the gas constant and T is the absolute temperature. The values of ΔG_{ads} values were presented in table 1. The negative value of ΔG_{ads} shows that the adsorption process is spontaneous. Generally, the mechanism of the adsorption process is categorized based on the value of ΔG_{ads} physisorption at around or below −20 kJ/mol which occurs as a result of the electrostatic interaction between inhibitor and metal surfaces [20]. The values of ΔG_{ads} around

-40 kJ/mol or less are characterized by the formation of covalent bonds (chemisorption mechanism) [25]. The value of ΔG_{ads} for this research indicates the physic sorption process.

D. Thermodynamic Parameters

The thermodynamic parameters of the corrosion process (i.e. Activation energy (Ea), enthalpy of activation (ΔH^0), and entropy activation (ΔS^0) in absence and presence inhibitors were calculated from Arrhenius equation, given in (4) and (6) [26].

$$C_r = Aexp\left(-\frac{E_a}{RT}\right) \tag{4}$$

where T is the absolute temperature and R is the universal gas.

$$logC_r = logA - \frac{E_a}{RT} \tag{5}$$

A plot of logC_r Vs 1/T gives a straight-line graph with intercept as logA and slope equal $-\frac{E_a}{R}$

The standard Entropy change ΔS^0 and standard Enthalpy changeΔH^0 of the reaction was calculated from the transition states form of Arrhenius equation given in (6):

$$C_r = \frac{RT}{Nh} exp\left(\frac{\Delta S^*}{R}\right)\exp\left(-\frac{\Delta H^*}{RT}\right) \tag{6}$$

Where Cr is corrosion rate from weight loss, A is the frequency factor, N is Avogadro's number and R is the universal gas constant. A plot of Log (Cr/T) against 1/T gives a straight-line graph with the slope of $-\frac{\Delta H^*}{RT}$ and intercept of $\log\left(\frac{R}{Nh} - \left(\frac{\Delta S^*}{R}\right)\right)$.

These parameters are used to understand the nature and mechanism of the corrosion process of mild steel. The results were presented in Table III, with the activation energy Ea of 11.33 KJ/mol, and 19.206kj/mol for a blank solution, and Cs-g-Paa respectively. The increase in the value of activation energy of the corrosion process upon the addition of an inhibitor indicates that the inhibitor hindered the reaction by increasing the energy barrier for the reaction process the higher the activation energy the less chance for the reaction to proceed. Furthermore, the increases in the entropy change of the reaction condition to more negative values in the blank solution to less negative values (in presence of Cs-g-Paa) show the decreases in the spontaneity of the reaction and directly reveal the inhibition performance. The corrosion in the blank solution shows more negative values and, upon the addition of an inhibitor, the value increased to less negative. This suggested that by the addition of an inhibitor we may control the spontaneity of the corrosion process. Positive values of enthalpy change indicate the corrosion of mild steel in 0.5MHCl is an endothermic process, this shows that by lowering the reaction temperature one may reduce the rate of the reaction. The result shows that the enthalpy change in the presence of Cs-g-Paa is higher than the blank solution having less enthalpy change.

TABLE III: THERMODYNAMIC PARAMETER

	ΔH ($Jmol^{-1}K^{-1}$)	ΔS ($Jmol^{-1}K^{-1}$)	ΔG (KJ/mol)	Ea (Kj/Mol)	R^2_1	R^2_2
Blank	53.97764732	-85.67454863	79.50866281	11.33302641	0.99913	0.99504
Cs-g-PAA	85.99245026	-85.59107607	111.4985909	19.20572012	0.99750	0.99471

E. Scanning Electron Microscopy (SEM) Analysis

The SEM image of mild steel coupon after immersion in corrosive media in the absence and presence of an inhibitor was presented in Fig. 4a and 4b respectively. It can be seen clearly that there exists pitting corrosion and roughness of the metal surface by the corrosive environment and there is the formation of different forms of corrosion products. The Comparative examination of these images, clearly suggest that the surface of mild steel is smoothened to a very large extent in the presence of inhibitor. This smoothening might be due to the adsorption of the inhibitor molecules on it and thus the surface is fully covered [27]. The rough surface with pits and cracks revealed that mild steel in the corrosive medium upon the addition of 500 ppm of Cs-g-PAA metal surface has become smoother and this indicates a surface film inhibitor is formed [28].

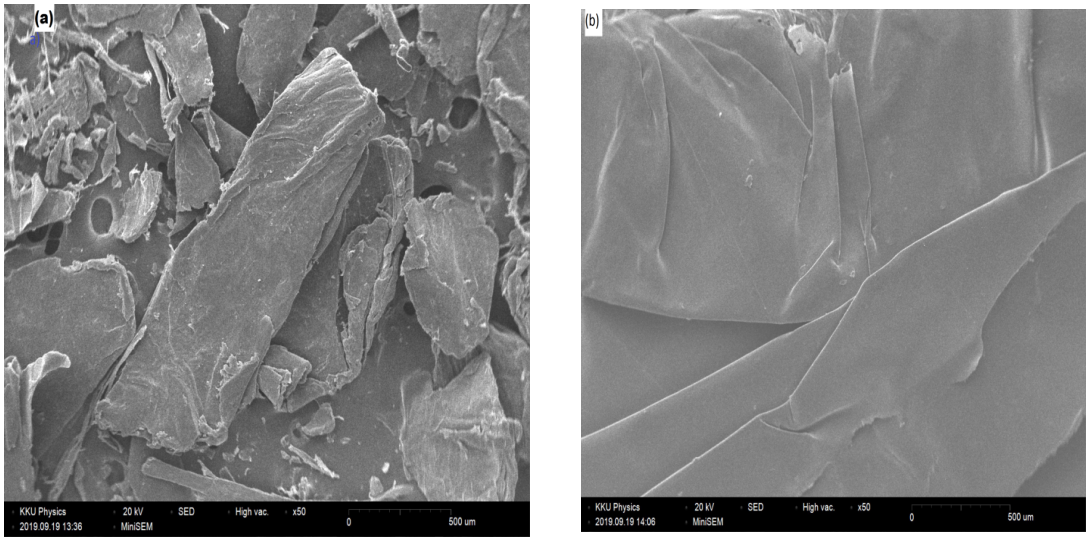

Fig. 4. SEM image of Mild steel after immersion in; a) absence of inhibitor, b) presence of inhibitor.

IV. Conclusion

Polyacrylic acid was successfully grafted on chitosan by a thermal method. The modified copolymer was characterized by different characterization methods. The corrosion inhibition efficiency of these polymers was tested on mild steel in 0.5M Hydrochloric acid by gravimetric. The inhibition mechanism was subjected to various adsorption models for which the result was best fitted with the Langmuir adsorption isotherm model with a correlation coefficient of 0. 9933. The results show high inhibition efficiency by the modified polymer in the order of 89- 94 at optimum conditions. Modified chitosan can serve as an alternative to corrosion mitigation methods.

Acknowledgment

The financial support from Khon Kaen University, Tetfund Nigeria, and Kano University of Science and Technology Wudil was highly acknowledged.

Conflict of Interest

The authors declare that they have no known competing financial interests or personal relationships that could have appeared to influence the work reported in this paper.

References

[1] Fathabadi HE, Ghorbani M, Mokarami Ghartavol H. Corrosion inhibition of mild steel with tolyltriazole. *Mater. Res.*, 2021; 24(4).
[2] Umoren SA, Solomon MM. Recent developments on the use of polymers as corrosion inhibitors-a review. *Open Mater. Sci. J.*, 2014; 8(1): 39–54.
[3] Erna M, Herdini H, Futra D. Corrosion Inhibition Mechanism of Mild Steel by Amylose-Acetate/Carboxymethyl Chitosan Composites in Acidic Media. *Int. J. Chem. Eng.*, 2019; 2019.
[4] Abd El-Salam HM, Kamal EHM, Ibrahim MS. Synthesis and Characterization of Chitosan-Grafted-Poly(2-Hydroxyaniline) Microstructures for Water Decontamination. *J. Polym. Environ.*, 2017; 25(4): 973–982.
[5] Khairkar SR, Raut AR. Synthesis of Chitosan-graft-Polyaniline-Based Composites. *Am. J. Mater. Sci. Eng.*, 2014; 2(4): 62–67.
[6] Nazifi DS, Modu KA, Mahmoud AA, Adamu HM. Ultrasonic Assisted Synthesis And Characterization Of Chitosan Graft With 2- (Dimethylaminoethylmethacrylate) (Dmaema) Cs-G-Pdmaem. *J. Phys. Sci.*, 2021; 3(1): 1–10.
[7] Salensky G. *Organic corrosion inhibitors*. in Corrosion Inhibitors, Principles and Recent Application. IntechOpen; 2018: 1–33.
[8] Mohammed S, Usman B. Investigation of Corrosion Inhibition potential of Ethanol Extract of Balanites aegyptiaca Leaves on Mild Steel in 1 M Hydrochloric Acid Solution. *Moroccan J. Chem.*, 2019; 07(3): 82–97.
[9] Dagdag O, Safi Z, Hsissou R, Erramli H, El Bouchti M, Wazzan N, Guo L, *et al.* Epoxy pre-polymers as new and effective materials for corrosion inhibition of carbon steel in acidic medium: Computational and experimental studies. *Scientific Reports*, 2019; 9(1): 1–14.
[10] Aljeaban NA, Goni LKMO, Alharbi BG, Jafar Mazumder MA, Ali SA, Chen T, Quraishi MA, *et al.* Polymers Decorated with Functional Motifs for Mitigation of Steel Corrosion: An Overview. *International Journal of Polymer Science*, 2020: 1-23.
[11] Wang W, Meng Q, Li Q, Liu J, Zhou M, Jin Z, Zhao K. Chitosan Derivatives and Their Application in Biomedicine. *International Journal of Molecular Sciences*, 2020; 21(2): 487. DOI: 10.3390/ijms21020487.
[12] Xuan Du D, Xuan Vuong B, Mai HD. Study on Preparation of Water-Soluble Chitosan with Varying Molecular Weights and Its Antioxidant Activity. *Advances in Materials Science and Engineering*, 2019; 2019: 1–8. DOI: 10.1155/2019/8781013.
[13] Meng J, Cui J, Yu S, Jiang H, Zhong C, Hongshun J. Preparation of aminated chitosan microspheres by one-pot method and

their adsorption properties for dye wastewater. *R. Soc. Open Sci.*, 2019; 6(5).
[14] Ziegler-Borowska M, Chełminiak D, Kaczmarek H, Kaczmarek-Kędziera A. Effect of side substituents on thermal stability of the modified chitosan and its nanocomposites with magnetite. *J. Therm. Anal. Calorim.*, 2016; 124(3): 1267–1280.
[15] Arora S, Lal S, Kumar S, Kumar M, Kumar M. Comparative degradation kinetic studies of three biopolymers: Chitin, chitosan and cellulose. *Arch. Appl. Sci. Res.*, 2011; 3(3): 188–201.
[16] Srivastava, Kumar R. Synthesis and Characterization of Acrylic Acid-g-(-Carrageenan) Copolymer and Study of Its Application. *Int. J. Carbohydr. Chem.*, 2013; 2013(May 2016): 1–8.
[17] Daniyal WMEMM, Fen YW, Saleviter S, Chanlek N, Nakajima H, Abdullah J, Yusof NA. (2021). X-ray Photoelectron Spectroscopy Analysis of Chitosan–Graphene Oxide-Based Composite Thin Films for Potential Optical Sensing Applications. *Polymers*, 2021; 13(3): 478. DOI: 10.3390/polym13030478.
[18] Taketa TB, dos Santos DM, Fiamingo A, Vaz JM, Beppu MM, Campana-Filho SP, Cohen RE, *et al.* Investigation of the Internal Chemical Composition of Chitosan-Based LbL Films by Depth-Profiling X-ray Photoelectron Spectroscopy (XPS) Analysis. *Langmuir*, 2018; 34(4): 1429–1440. DOI: 10.1021/acs.langmuir.7b04104.
[19] Chauhan DS, Srivastava V, Joshi PG, Quraishi MA. PEG cross-linked Chitosan: a biomacromolecule as corrosion inhibitor for sugar industry. *Int. J. Ind. Chem.*, 2018; 9(4): 363–377.
[20] Idouhli R, Koumya Y, Khadiri M, Aityoub A, Abouelfida A, Benyaich A. Inhibitory effect of Senecio anteuphorbium as green corrosion inhibitor for S300 steel. *Int. J. Ind. Chem.*, 2019; 10(2): 133–143.
[21] Yadav M, Sharma U, Yadav PN. Isatin compounds as corrosion inhibitors for N80 steel in 15% HCl. *Egypt. J. Pet.*, 2013; 22(3): 335–344.
[22] Alaba O, Johnson O, Leke E. Results in Materials Thermodynamics and adsorption study of the corrosion inhibition of mild steel by Euphorbia heterophylla L . extract in 1 . 5 M HCl. *Results Mater.*, 2020; 5(November 2019): 100074.
[23] Verma C, Kumar AM, Mazumder MAJ, Quraishi MA. Chitosan-Based Green and Sustainable Corrosion Inhibitors for Carbon Steel. *Intech*, 2016; 1(3): 144–156.
[24] Gowri S, Sathiyabama J, Rajendran S. Corrosion inhibition effect of carbon steel in sea water by L-Arginine-Zn2+ system. *Int. J. Chem. Eng.*, 2014; 2014(1).
[25] Eddy NO, Momoh-Yahaya H, Oguzie EE. Theoretical and experimental studies on the corrosion inhibition potentials of some purines for aluminum in 0.1 M HCl. *J. Adv. Res.*, 2015; 6(2): 203–217.
[26] Banera US, Gervasi MJ, Gervasi C.Inhibition of mild steel corrosion in HCl solution using chitosan Inhibition of mild steel corrosion in HCl solution using chitosan. *Cellulose*, 2013; (10).
[27] Nicho PM, Ramirez-Arteaga AM, Diaz EF, Valenzuela E, Serna S. Poly(Acrylic Acid) and Potassium Sodium Tartrate as Effective Corrosion Inhibitors for Mild Steel in Aqueous Environment. *J. Adv. Electrochem.*, 2016; 2(4): 136–140.
[28] Kumari PM, Lavanya M, Rao SA. Corrosion Inhibition of Mild Steel in Acidic Media by N-[(3,4-Dimethoxyphenyl) Methyleneamino]-4-Hydroxy-Benzamide. *J. Bio- Tribo-Corrosion*, 2021; 7(1): 1–19.